Use of C-surface based force-feedback algorithm for complex assembly tasks

J-P. Merlet
INRIA Sophia-Antipolis
2004 Route des Lucioles
06665 Valbonne Cedex
France
E-mail: merlet@cygnusx1.inria.fr

Abstract
We describe the principle of a force-feedback controller based on the C-surface theory. Experimental results on complex assembly tasks are presented and we compare various force-feedback strategies. We show that our force-feedback algorithm can perform these tasks with few a-priori informations and can be used to learn a reference trajectory.

1 Introduction

1.1 Hybrid control

Hybrid control [3] is probably one of the most efficient force-feedback control scheme. In this scheme the configuration space of the task is partitioned in directions where pure positional control is used and directions where there is only force-control (i.e. the input of the control law is the force measurements). In the classical implementation of this scheme [1] the operator has first to choose a configuration space (i.e. a set of parameters necessary to describe the task), a compliance frame in this configuration space and to determine which kind of control is to performed along each direction of this frame, either positional control or force control. Therefore the operator has to determine a *selection matrix* which is diagonal and whose diagonal element is 1 if the direction is force-controlled and 0 otherwise. To obtain good performances with this kind of implementation some assumptions are necessary :

- existence of the compliance frame
- the compliance frame is perfectly known.
- the relation between the contact forces[1] and the positional errors of the manipulator is one-to-one

For simple tasks these assumptions may be verified (for example if the end-point of the robot has to follow a fixed plane). However, even in these simple cases, small errors may yield to an unstable behavior of the robot (for example if the position of the plane is slightly different from its model). Furthermore it has been shown that the compliance frame may be not defined for some tasks [3] or that its position is time-dependent (for example when the robot has to follow an unknown shape). Various tasks for which the assumption about the one-to-one mapping between the force measurements and the positional errors is clearly false has been given in [4].

1.2 Hybrid control with the C-surface theory

The drawbacks of the classical hybrid control scheme can be suppressed by computing the compliance frame according to the informations obtained from the task i.e. from the forces measurements. We have proposed such a method in [5], based on the C-surface theory developed by Mason. Let us consider a configuration space which dimension is equal to the number of degree of freedom necessary to perform the task (we will consider that this dimension is at most

[1] In this paper forces will mean forces and torques

6). In this configuration space the manipulator (or the part it moves) is represented by a point P. According to the task the configuration space can be divided into the *free space* where there is no contact between the object grasped by the manipulator and the surrounding and the *contact space* where there is a contact. The frontier between these two volumes is called the *C-surface* of the task. Clearly the only possible motion of point P when there is contact is to slide on the C-surface (we assume that the deformations of the objects can be neglected). Locally this motion occurs along the tangent hyperplane of the C-surface. At the opposite a motion of P along the C-surface normal unit vector $\mathbf{N}$ yield to an increase or a decrease of the contact forces. Therefore from the hybrid control view point the C-surface normal is the direction of the configuration space on which a pure force control is necessary and at the opposite a positional control is necessary along the tangent hyperplane. Therefore the determination of the C-surface normal $\mathbf{N}$ enables to determine both the compliance frame and the selection matrix. This normal can be estimated geometrically if the task is fully specified but in most real tasks the models errors will be to great to ensure a correct control. Thus a better way to calculate $\mathbf{N}$ is to use the force measurements. Indeed we have shown in [4] that the forces measurements vector is exactly the C-surface normal if the velocity of the manipulator is sufficiently low (which will be the case for the tasks considered in this paper). Therefore the force measurements enables to measure locally the C-surface normal.

1.3 Principle of a C-surface based hybrid controller

The configuration space is determined by a set $\mathbf{X}$ describing the position of the manipulator (or the object it grasps) and a set $\mathbf{\Omega}$ of angular positions. Let us assume that the desired velocity of the manipulator (i.e. the magnitude of $\dot{\mathbf{X}}$) is V_d, the maximum angular velocity (i.e. the magnitude of $\dot{\mathbf{\Omega}}$) is ω_m, the desired force and torque magnitude F_d, M_d. The force measurements vector is $\mathbf{F_m}$ and is divided in its force and torque componants $\mathbf{F_m^X}$ and $\mathbf{F_m^\Omega}$. An initial velocity $\dot{\mathbf{X}}_\mathbf{i}$ is given at the beginning of the task. According to our assumption we have during a contact:

$$\mathbf{N} = [\mathbf{N_X} \quad , \quad \mathbf{N_\Omega}]^T = \left[\frac{\mathbf{F_m^X}}{||\mathbf{F_m^X}||} \quad , \quad \frac{\mathbf{F_m^\Omega}}{||\mathbf{F_m^\Omega}||} \right]^T \tag{1}$$

A control law along $\mathbf{N}$ ensures the regulation of the magnitude of the force. For example a proportional control law can be used with:

$$\dot{\mathbf{X}}_\mathbf{N} = k_p^X(||\mathbf{F_m^X}|| - F_d)\mathbf{N_X} \quad \text{with} \quad ||\dot{\mathbf{X}}_\mathbf{N}|| \leq V_d \tag{2}$$

$$\dot{\mathbf{\Omega}}_\mathbf{N} = k_p^\Omega(||\mathbf{F_m^\Omega}|| - M_d)\mathbf{N_\Omega} \quad \text{with} \quad ||\dot{\mathbf{\Omega}}_\mathbf{N}|| \leq \omega_m \tag{3}$$

where k_p^X, k_p^Ω are gains. From the value of $\mathbf{N}$ we are able to determine a vector $\mathbf{T}$ in the tangent hyperplane of the C-surface such that a motion along this vector will satisfy a goal given by the operator. We have:

$$\mathbf{T} = [\mathbf{T_X} \quad , \quad \mathbf{T_\Omega}]^T \tag{4}$$

The velocity along $\mathbf{T_X}$ and the angular velocity along $\mathbf{T_\Omega}$ will be :

$$\dot{\mathbf{X}}_\mathbf{T} = (\sqrt{V_d^2 - ||\dot{\mathbf{X}}_\mathbf{N}||^2})\mathbf{T_X} \tag{5}$$

$$\dot{\mathbf{\Omega}}_\mathbf{T} = (\sqrt{\omega_m^2 - ||\dot{\mathbf{\Omega}}_\mathbf{N}||^2})\mathbf{T_\Omega} \tag{6}$$

The desired velocities of the manipulator are given by :

$$\dot{\mathbf{X}} = \dot{\mathbf{X}}_\mathbf{T} + \dot{\mathbf{X}}_\mathbf{N} \qquad \dot{\mathbf{\Omega}} = \dot{\mathbf{\Omega}}_\mathbf{T} + \dot{\mathbf{\Omega}}_\mathbf{N} \tag{7}$$

In the case where the magnitude of $\mathbf{F_m^X}$ is too low we will have :

$$\dot{\mathbf{X}} = \dot{\mathbf{X}}_\mathbf{i} \tag{8}$$

A problem may arise when the C-surface normal is not unique, for example when P lie on an edge of the C-surface. In that case the motion resulting from our scheme may yield either to some disturbance of the force signal or to loose the contact with the C-surface. In the first case the disturbance will disappear as soon as point P leaves the edge of the C-surface. In the second case either the velocity $\dot{\mathbf{X}}_\mathbf{i}$ enables to perform correctly the task or a new contact will appear.

2 Experimental results

2.1 The test-bed

The purpose of our experiments is the assembly of parts of a washing machine. The test-bed can be seen on Figure 1. The robot is an IBM 7576 Scara robot with a parallel manipulator as a wrist (in these experiments this wrist is used only to ensure some passive compliance to the robot). The parts are fixed on a table which lie on an AICO 6 componants force sensor. The robot is controlled through an AICO controller with 3 CPU. The experimental programs are written in C on a SUN workstation and downloaded through a serial link in the controller. The sampling rates of the position loop of the robot and the force measurement are 5ms.

Figure 1: The assembly test-bed. We use an IBM 7576 Scara robot with a parallel manipulator as a wrist. The parts are fixed on a table which lie on an AICO 6-componants force sensor.

2.2 Preliminary experiment

A first experiment was necessary to calibrate the force sensor i.e. to find the position of the force sensor frame with respect to the robot frame in order to get the force measurements in this last frame. At the same time our purpose was to verify our assumption about the relation between the C-surface normal and the force vector.

For this purpose a ruler is fixed on the table and the robot is programmed so that it hits the ruler at various points (the contact was detected by the force sensor). At each point the current position of the robot together with the force measurements are recorded. We assume that we know the position of the center of the force sensor in the robot frame and that both z axis of the force sensor and robot frame are parallel: under these assumptions the calibration unknown is the rotation angle α between the two frames. A least-square algorithm is used to find the equation of the line associated to the ruler and from this equation we deduce the normal vector $\mathbf{N}$ to the ruler. Our basic assumption is that the force measurement vector is perpendicular to the ruler. To verify this assumption we use another least-square algorithm to find the rotation angle α which ensure that a criteria J is minimized with:

$$J = \sum_{i=1}^{i=n} ||R(\alpha)\frac{\mathbf{F_i}}{||\mathbf{F_i}||} - \mathbf{N}||^2$$

where n is the number of contact points, $\mathbf{F_i}$ the force vector at contact point i and $R(\alpha)$ the rotation matrix of angle α around the z axis. If our assumption is verified this criteria will be low at the end of the process. The robot hits the ruler at ten contact points and after completion of the least square algorithm the value of J is 0.072555. The angles between $\mathbf{N}$ and the force vector at each contact point are given in the following table.

Point	1	2	3	4	5	6	7	8	9	10
Angle	6.4664	-0.4738	2.7	2.6067	-2.8425	2.1147	-1.4375	-4.0476	-2.0729	-3.0375

Their average value is -0.002398 degree and the standard deviation is 3.172530 degree. The very small average value shows that our basic assumption seems to be reasonable.

2.3 Phase 1 : Assembly of the filter and the plug

These two parts are described in Figure 2. This operation is a zero-clearance assembly task because the diameter of the hole in the plug is less than the distance between the two pins on the filter. Therefore this assembly can be performed only by using the elasticity of these pins.

2.3.1 Assembly with a guarded move strategy

The plug can be grasped either along its diameter or along its normal which yield to either an horizontal insertion axis or a vertical one. However it may be noticed that the second way is more appropriate in the sense that the forces acting on the plug will lie mostly along its normal and therefore will be counterbalanced by the whole stiffness of the robot. In a first experiment we decide to perform this assembly by using a guarded move strategy along the vertical axis. The desired force value is greater than the force necessary to deform the pins. Under these conditions the assembly will be completed (provided that the lateral misalignments are not too large) and the robot will stop when the plug reaches the front part of the filter.

Experimental results are presented in Figure 3. If we consider the plot of the force along the z axis we notice a first increase corresponding to the deformation of the pins (the necessary force is approximatively 80 N). As soon as the insertion is performed the elastic energy stored in the wrist yields to an upward-downward motion of the plug which hits the pins (time=28) causing a change of sign of the F_z signal. But the damping is strong and at time 37 there is a decrease of the force while the robot is now moving the plug toward the front part of the filter. Then the plug hits this front part (time=80) and the robot moves downward until the desired force (100 N) is obtained.

We notice that the positionning errors along the axis perpendicular to the insertion axis are approximatively 2 mm and are corrected by the passive compliance behaviour of the parallel wrist. Here the insertion axis given by the operator is quite accurate and therefore the lateral forces remain small. In that case the guarded move strategy is quite efficient : failures have been observed only when the distance between the initial position of the robot and the insertion axis was greater than 3 mm.

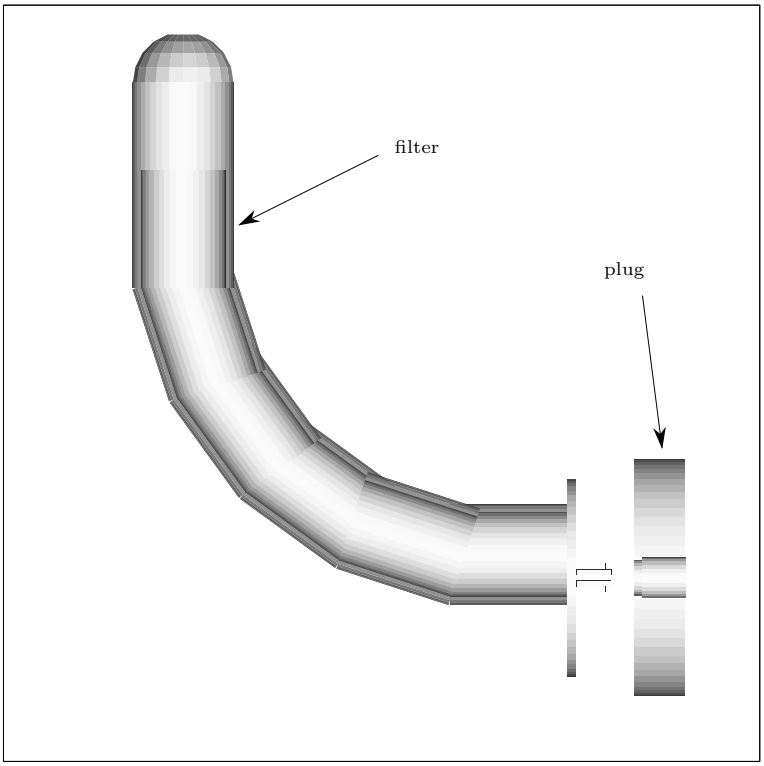

Figure 2: Phase 1. The plug, the filter and the manifold.

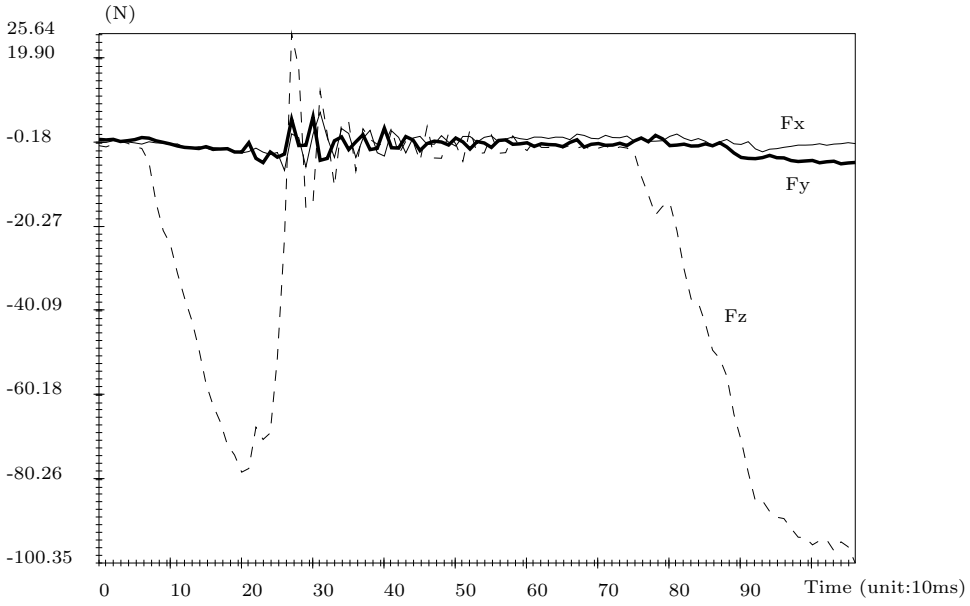

Figure 3: Phase 1, assembly of the plug and the filter. Positions of the gripper and contact forces during the assembly with passive compliance, guarded move strategy and vertical insertion axis.

2.3.2 Assembly with active compliance

For this task we may assume that the parts have the same orientation. Therefore only the x, y, z are to be controlled. The large clearance enables to use an hybrid control with a fixed compliance frame where all three axis are force-controlled with a zero desired force along x, y and a positive value along z, greater than the force necessary to deform the pins. The parameters of our controller are the desired force value and a proportional gain relating the variations of the lateral motions according to the values of the lateral forces.

Experimental results are presented in Figure 4. According to these results we notice some interesting points concerning the use of the force feedback algorithm. During the initial contact (time=0-10) small misalignments of the plug along the x, y axis are corrected. After the assembly the forces F_x, F_y are smaller than with the guarded move strategy. During the downward motion of the robot these small forces are used to slowly correct the position of the plug. At time 75 the misalignments are quite equal to zero and from this point there is no lateral motion of the plug. It must be noticed that both lateral forces are very close to zero and are better controlled around this value than with the guarded move strategy. At time 100 the plug hits the front part of the filter yielding to small variations of the position of the plug along the lateral axis. During our experiments no failure have been observed although initial errors of up to 4 mm have been introduced. As a matter of conclusion the active compliance scheme yields to a more robust controller with respect to the lateral misalignments of the plug.

2.4 Phase 2: Assembly of the filter in the manifold

The filter can be seen on Figure 2 and the manifold on Figure 1. There are large clearances between these two parts: 3.5 and 6.0 mm. If the grasping position of the filter and the position of the manifold is well known an off-line motion planning strategy may be used to determine the trajectory of the robot. We assume here that these data are not available and that the only a-priori informations are:

- an initial position of the filter such that its extremity is close from the entry of the hole in the manifold.

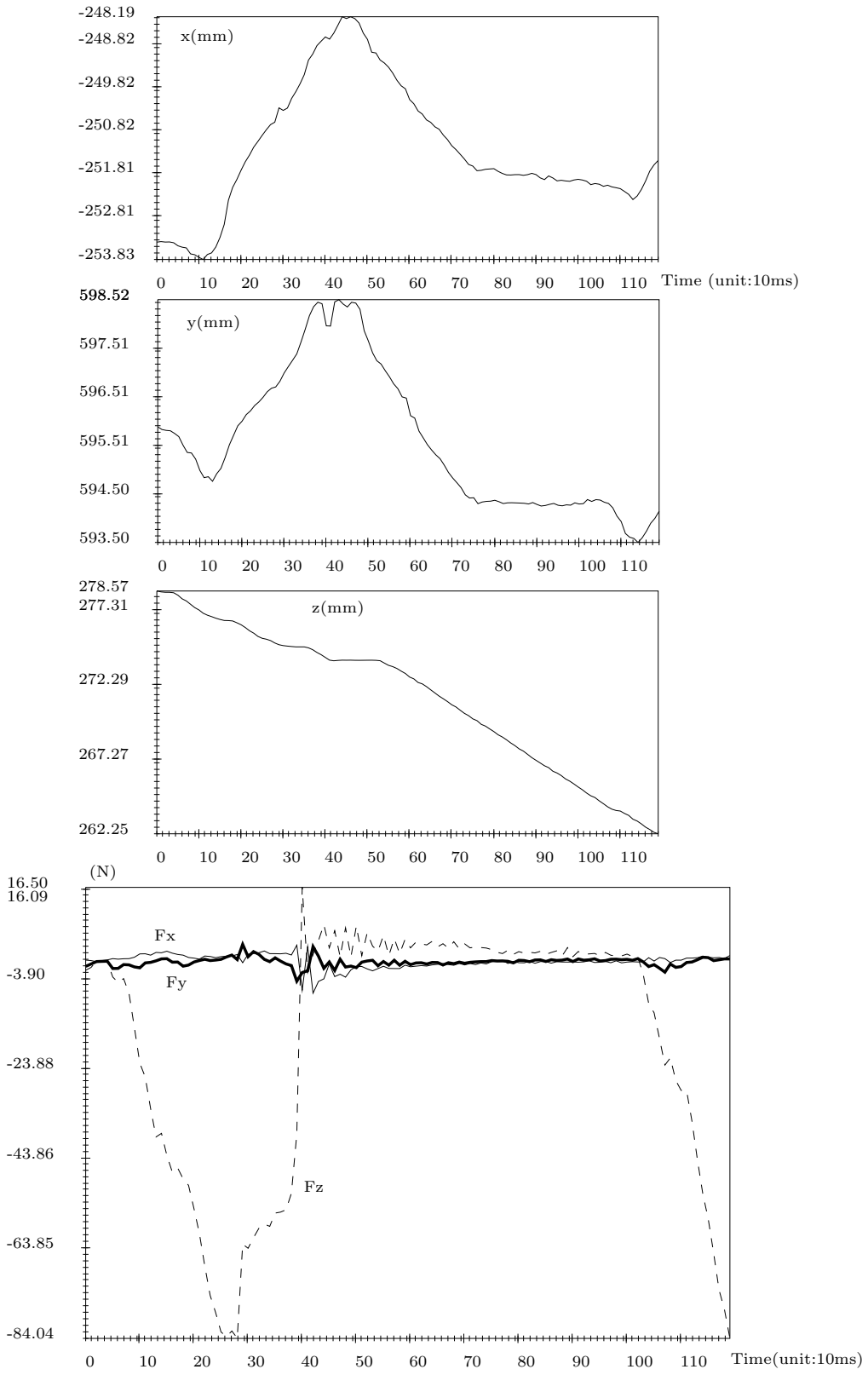

Figure 4: Phase 1, assembly of the plug and the filter. Positions of the gripper and contact forces during the assembly with active compliance, free wrist and vertical insertion axis.

- a rough estimate of a direction vector enabling to put the extremity of the filter inside the hole.

Our purpose is to complete this assembly whatever is the shape of the manifold. During this task the variables to be controlled are x, y, θ where θ is the rotation angle around the z axis of the Scara robot (we assume here that the coordinates z of the robot is constant during the task). For the hybrid control scheme we may see clearly that we cannot find here a fixed compliance frame. Less obvious is that expressing the compliance frame in the tool frame may yield to a failure of the task. It would seem natural to state that in the tool frame the axis corresponding to the general axis of the filter is to be position-controlled and that the perpendicular axis is to be force-controlled. This scheme will fail when the filter hits a part of the manifold where the normal lie approximatively along the axis of the filter (Figure 5). Note that our controller will succeed in this situation: it will first cause a backward motion along the axis of the filter in order to control the contact force and a lateral motion along the perpendicular axis and gradually the filter will move toward the entry of the hole.

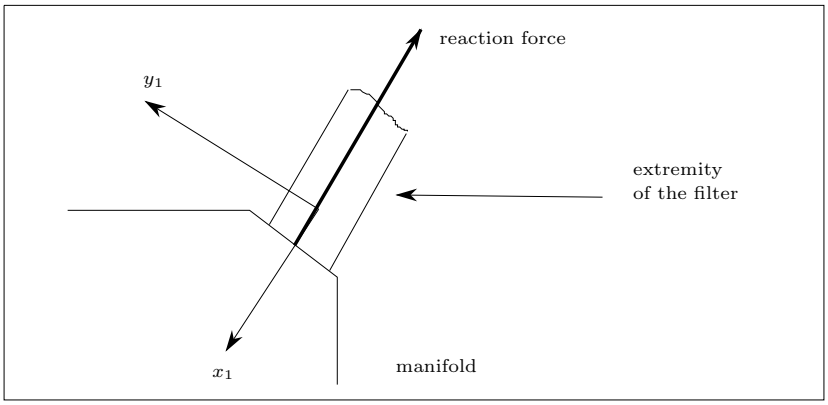

Figure 5: Assembly of the filter in the manifold. The compliance frame calculated in the tool frame may yield to a failure of the task.

In fact the compliance frame cannot be easily described in any frame and therefore we claim that the best estimation of the compliance frame is obtained from the force measurements. In our program the robot uses an internal position control loop at 10 ms which set the values of the articular coordinates used in the most internal position loop of the robot.

A problem may arise from the fact that there is not a one-to-one relation between the forces vector and the misalignments as illustrated in Figure 6. During step 1 the filter moves along the insertion axis until the filter hits the manifold at point A. The torque around the grasping point along the z axis is negative and consequently there is a negative rotation of the filter which yield to an increase of the orientation error. At this point the reaction force at A yields to a motion along the C-surface normal $\mathbf{N}$. These motions yield to a second contact point B at step 2 and consequently to a change of sign of the torque. The filter rotates around the grasping point and the orientation error is partially corrected. During step 3 the torque is small but there is a reaction force yielding to the centering of the filter with a lost of contact. At step 4 there is no more contact and the grasping point moves along the insertion axis until a new contact appears.

Therefore the problem is the bad correction of the orientation during step 1 of the assembly. This is mostly due to the initial bad orientation of the filter but in any case the algorithm corrects this error in the following steps of the assembly. For this experiment the filter is grasped on its body near its front part (our gripper does not enable to grasp the front part). The insertion is performed until the gripper hits the manifold. Figure 7 shows the record of the position of the robot, the contact forces and torque around the z axis during the assembly. We may notice on the θ record that the problem mentioned in the previous section occurs: there is a negative rotation of the wrist between

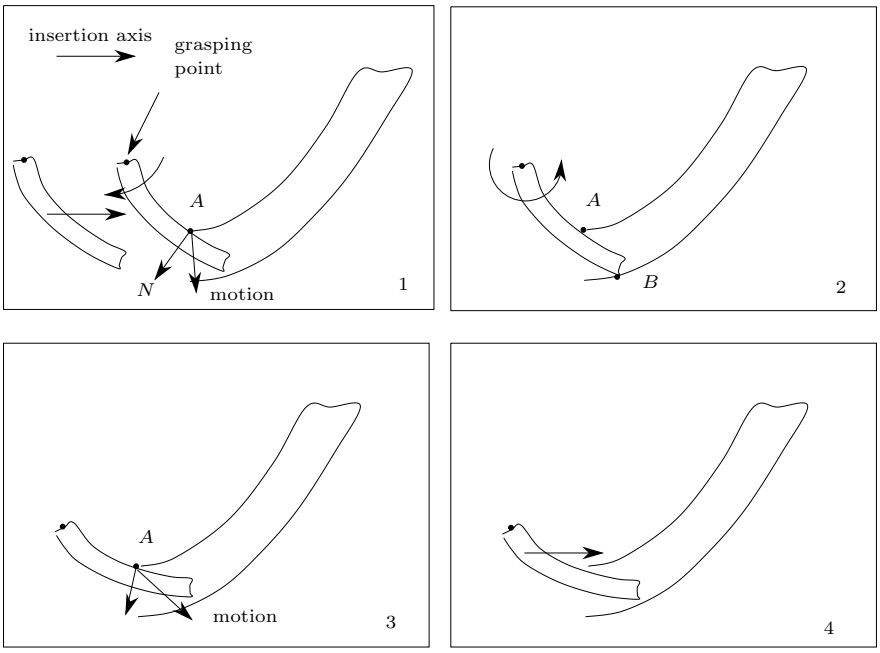

Figure 6: Assembly of the filter in the manifold. What my happen.

time 0 and 5. After this initial error the record shows that θ is approximatively a linear function of time which means that the followed trajectory is an arc of circle as it may be expected. We may notice that a force control along the z axis may be useful because although the z force is equal to zero at the beginning of the task great variations of this force may be observed during the assembly. Our assumption is that there is a small change in the grasping position due to the great length of the filter and the torque involved at the beginning of the assembly which yields to an error on the position along the z axis.

During time 0-10 the torque is effectively positive and became then negative until time 35. At this point the torque becomes positive which means that we are in the same situation as at the beginning of the assembly. Then the torque steps back to a negative value. A similar situation occurs at time 46. At the end of the assembly (time 72) the gripper is in contact with the manifold and the torque becomes constant. Note that the filter is always in contact with the manifold (except at time 33-34 and 45). This is due to the fact that we have no a priori knowledge of the trajectory: even in the case of a lost of contact between the parts the fixed insertion axis yields to a new contact a few steps after the lost of contact.

As a matter of conclusion this experiment enables to show that the force controller is able to perform complex assembly tasks even with few informations. For the considered assembly however a reference trajectory might be useful because a reference model of the assembly enables to get a better control of the contact force.

It is possible to build a reference trajectory for this assembly from the experimental data obtained after a first experiment. To calculate this reference trajectory we consider the set of points of the data for which the torque and force are small together with the last point (at this point the assembly is performed). These sets are used as control points to calculate a spline for each of the x, y, θ variables. Figure 8 shows the reference trajectory obtained for each variable. Figures 9 shows the forces and torque measured when the gripper described the reference trajectory in open loop. Note that until the gripper hits the manifold (time 499) the forces are very small. The average values of F_x, F_y are 0.0795 N, 0.3067 N and their standard deviation is 0.293 N and 0.368 N. We see on the torque plot that at time 499 there is a one contact point between the filter and the manifold. Then the filter rotates around this point until

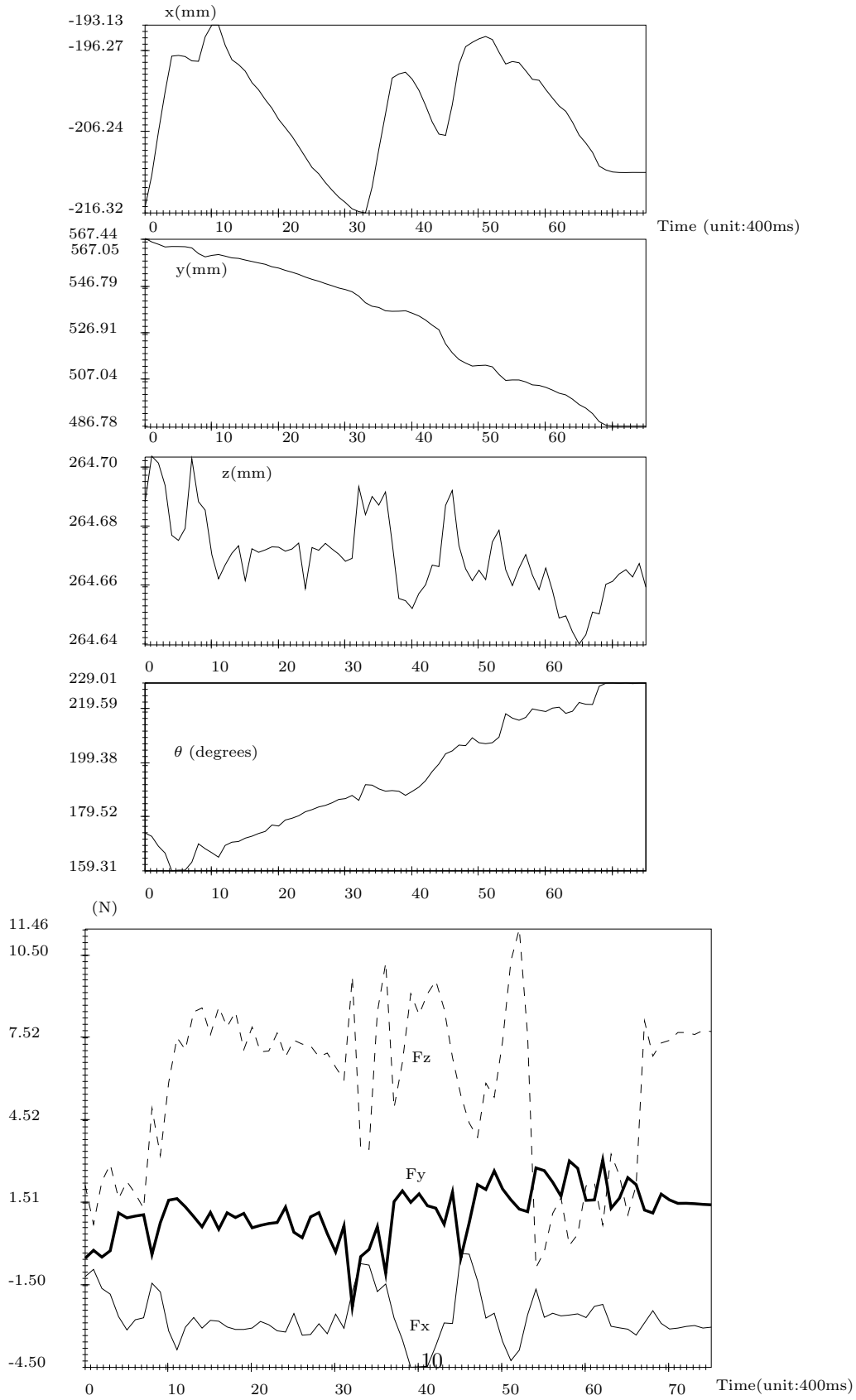

Figure 7: Phase 2: assembly of the filter in the manifold. Positions of the robot, contact forces and torque during the assembly with active compliance, free wrist and vertical insertion axis. Note that the torque is the torque exerted by the robot and therefore the opposite of the torque used by the force-feedback algorithm.

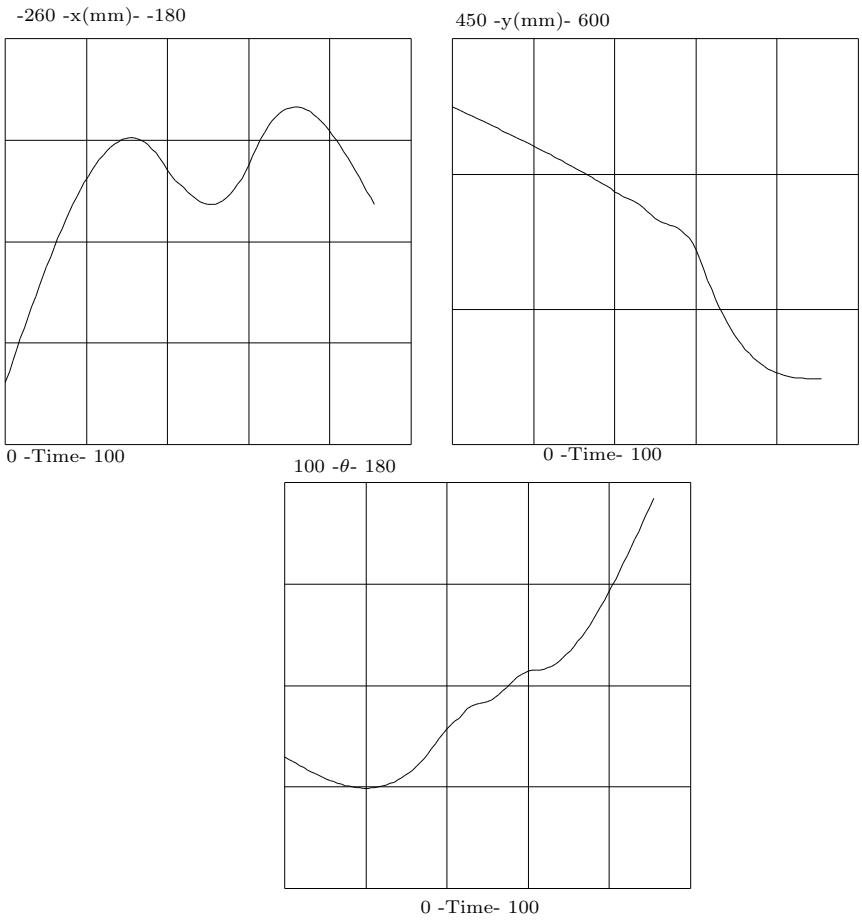

Figure 8: Phase 2: assembly of the filter in the manifold. Reference trajectory of the gripper obtained from the previous data.

the gripper is applied against the front of the manifold yielding to a continuous increase of the torque.

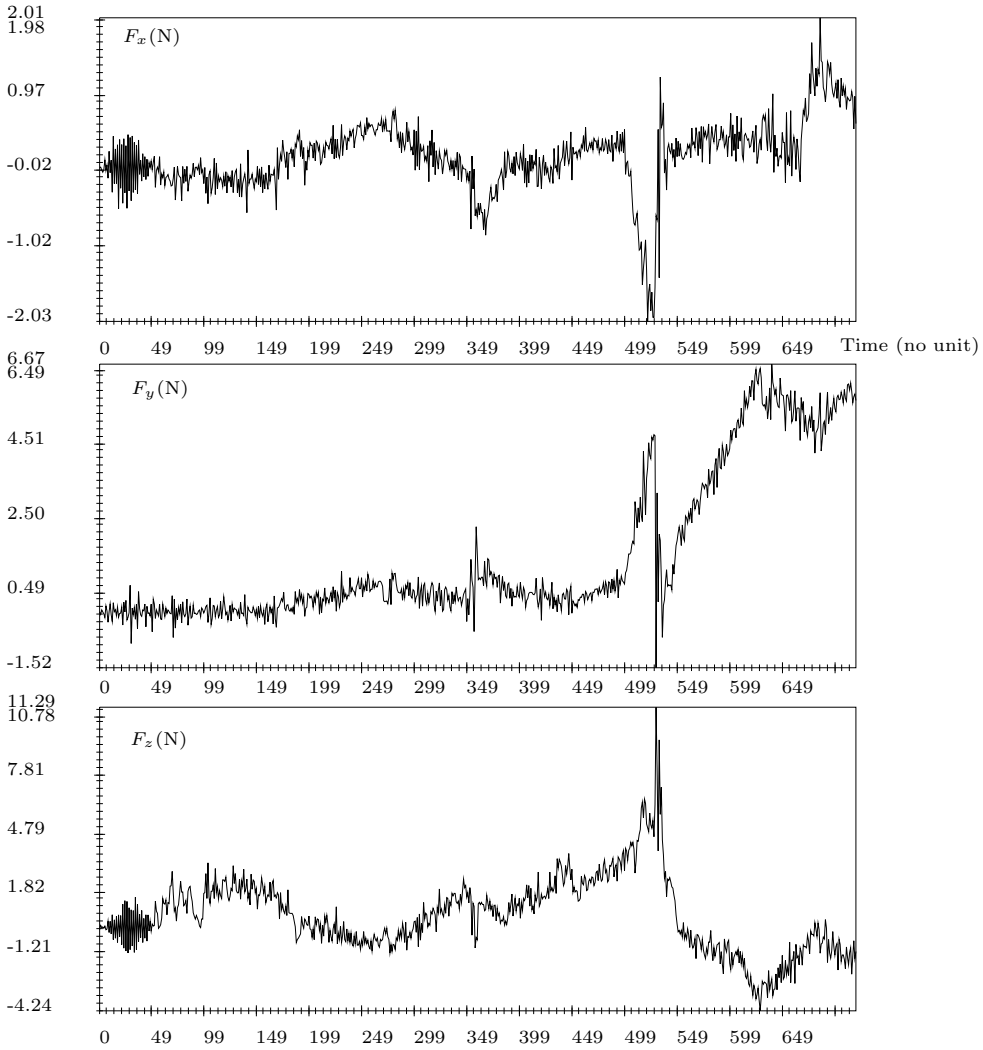

Figure 9: Phase 2: assembly of the filter in the manifold. Force and torque measurements obtained for the reference trajectory of the gripper followed in an open-loop mode.

2.5 Phase 3: Assembly of the pump motor in the manifold

The lodging of the pump motor may be seen in Figure 2. The grasping is performed in such a way that the center of the gripper lie on the same vertical axis as the cylinder of the pump motor. This is a two insertions assembly task : one prismatic insertion of the motor in a slide and a cylindrical insertion. These insertions are not synchronous: the insertion in the slide occurs before the cylindrical insertion. Experimental results obtained with the force-feedback algorithm used in Phase 1 are presented in Figure 10. Note that the lateral misalignments are corrected during the insertion (between time 0-70). At time 70 the cylindrical insertion begins and causes a small disturbance on the lateral position which is rapidly corrected (time 85). Note also that a large vertical axis force is necessary at the end of the

task to complete the insertion (more than 10 N). As a matter of conclusion we have noticed one case of failure during

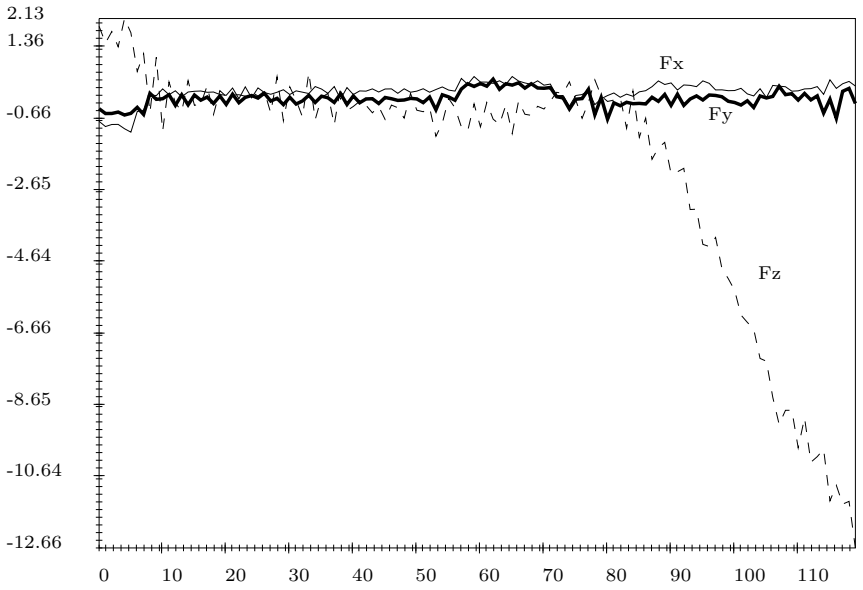

Figure 10: Phase 3: Assembly of the pump motor. Positions of the gripper and contact forces during the assembly with active compliance, free wrist and vertical insertion axis

the experiment. It was due to the presence of plastic dusts in the slide of the manifold which reduce greatly the clearance of the parts. A consequence was that the F_z force necessary to perform the assembly was much more higher than in the normal task. As the z axis of the gripper is different from the z axis of the slide a large torque was applied and creates a deformation of the slide. When the motor comes close to the cylinder of the manifold there was a large orientation error which cannot be corrected by a translation of the gripper. Therefore it may be necessary also to control the torques during this task to avoid this kind of failure but in the present state of the test bed this cannot be done. However for a more normal state of the parts the force-feedback algorithm was efficient.

2.6 Phase 4: Screwing of the plug in the manifold

In this phase the grasping position is identical to the one in Phase 1 and the insertion axis of the plug is vertical. Note that the grasping position is such that there is a small distance between the z axis of the gripper and the z axis of the plug and therefore an open loop control will be inefficient. The x, y, z axis are force controlled : the two first one are controlled through the C-surface theory and the z axis is independently controlled. The motion along the x, y axis enables to correct the misalignments of the gripper with the axis of the plug. If the forces along the x, y axis are sufficiently small a one axis proportional regulator is used to control the F_z force. If this force is close from the desired value (here 6N) a rotation of the gripper is performed. Although the range of the rotation axis of the robot is too small to fully perform the screwing it has been possible to show that the screwing was effective.

Experimental results are presented in Figure 11. We see clearly on the position records that there was first a correction of the misalignments of the parts at the beginning of the task together with a large motion along the z axis in order to obtain the desired force value (time 0-10). After that the screwing proceeds rather smoothly (the θ record shows that the screwing speed is quite constant) with a screwing rotation of 150°. Due to the distance between the z axis of the robot and the z axis of the plug we may expect the forces along the x, y axis to be theoretically a sine curve as it can be observed on the force records. Note also on this figure the record of the force F_z which value is

always close from the desired value in spite of the disturbances involved by the screwing motion.

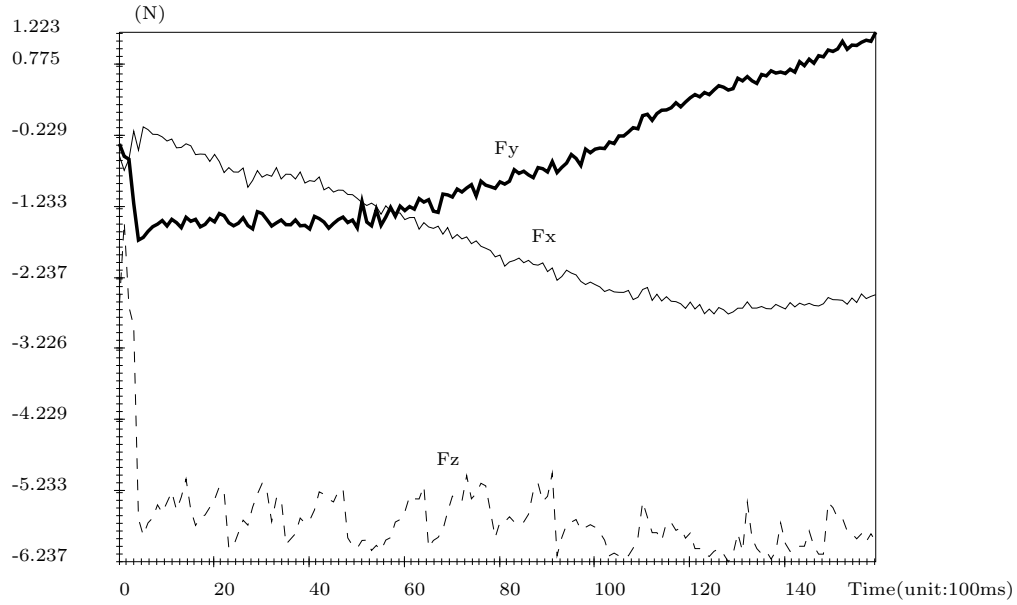

Figure 11: Phase 4: Screwing of the plug. Positions of the gripper and contact forces during the assembly with active compliance, free wrist and vertical insertion axis.

3 Conclusion

It may seem obvious that some of the assembly tasks presented in this paper can be performed in open loop (for example the assembly involved in Phase 2) but this assumption will be true only if the robotics cell is highly structured. The main problem is the grasping of the different parts involved in the assembly. We may fear that the variation in the shape of the parts and their flexibility can induce large grasping errors yielding to failure of the assemblies. Thus the need of a force sensor to detect the failure is clearly established.

In our case the test bed is not really structured: the initial position of the parts at the beginning of the assembly are determined "by hand" and this yields to rather large errors. We have also chosen to use only high-level primitives which can deal with a broad range of application and are not specific to the considered tasks. In order to use these primitives for this specific application one has to determine at most a few set of parameters : the insertion axis vector (which can be only a rough estimate) and one or two gains which are mainly related to the material of the parts and not to the assembly. We may thus expect that after a few trials a set of parameters usable for a broad range of assembly tasks will be determined.

As for the force controller we have shown that the most classical approach (i.e. guarded move strategy and hybrid control with a fixed compliance frame) may work for some of the assemblies but will fail for others. This is clearly due to the fact that the basic assumptions on which are based these approaches are not verified (especially for the Phase 2). However it may be useful to design high-level primitive of this type to deal with the most simple applications.

At the opposite of these simple strategies we have shown that our force-feedback controller is very efficient and has a broad range of application. The records presented in this paper show clearly that it can deal with very various assembly tasks as shown in [5].

Another important point is that a more precise control of the forces and torques will ensure a better quality of the assembly together with a decrease of the number of failure case.

Our next step will be to implement our force-feedback controller on our active wrist prototype. Although this macro-micro manipulator approach has been studied by some authors ([6],[2]) we intend to test it with a more efficient micro-manipulator and for a broader range of applications.

References

[1] Craig J.J., Raibert M.H. "A systematic method of hybrid position- force control of a manipulator", J. of Dyn.Sys. , Meas. and Control , 1981 , 103, 2 , pp.126-133

[2] Khatib O. "Reduced Effective Inertia in Macro/Micro Manipulator Systems", 5th ISRR, Tokyo, August 28-31,pp. 329-335.

[3] Mason M.T. "Compliant motion" in Robot , Motion-Planning and Control, Brady & al Ed.,Cambridge , The MIT Press, 1982

[4] Merlet J-P. "Contribution à la formalisation de la commande par retour d'efforts. Application à la commande de robots parallèles" PhD thesis, Univ. Paris VI, June 18, 1986

[5] Merlet J-P. "C-surface theory applied to the design of an hybrid force-position robot controller" IEEE Int. Conf. on Robotics and Automation, Raleigh, North Carolina, March 30-April 3,1987

[6] Reboulet C., Robert A. "Hybrid control of a manipulator with an active compliant wrist", 3th ISRR, Gouvieux, France, Oct. 7-11, 1985, pp.76-80